Journal of Environmental Radioactivity 175-176 (2017) 15–24

Contents lists available at ScienceDirect

Journal of Environmental Radioactivity

journal homepage: www.elsevier.com/locate/jenvrad

East Urals Radioactive Trace: Dose-dependent functional-metabolic effects in the myocardium of the pygmy wood mouse (*Apodemus uralensis*) taking into account population size

Natalýa A. Orekhova*, Makar V. Modorov

Institute of Plant and Animal Ecology, Ural Division of Russian Academy of Sciences, 8 Marta street, 202, Ekaterinburg, 620144 Russia

ARTICLE INFO

Article history:
Received 22 September 2015
Received in revised form
26 February 2017
Accepted 6 April 2017

Keywords:
EURT
Rodent
Myocardium
Functional-metabolic radiation effect
Population abundance
Radiometric data

ABSTRACT

The population dynamics, radiometric data and biochemical parameters (concentrations of total lipids, proteins, DNA and RNA, activity of succinate dehydrogenase, glucose phosphate isomerase and catalase, as well as lipid peroxidation level) in the myocardium of the pygmy wood mouse (*Apodemus uralensis* Pall., 1811) inhabiting the area of the East Urals Radioactive Trace (EURT) were analyzed. The functional-metabolic radiation effects as a result external and internal exposure to ^{137}Cs and ^{90}Sr (unweighted total dose rate 0.04–0.5 mGy/day) are characterized by a reduction in lipid catabolism, mitochondrial oxidation and antioxidant defense, as well as the activation of anaerobic glycolysis as well as the protein-synthesizing and genetic apparatus. The data indicate the low efficiency of cell energy production and allow us to state that compensatory myocardial hypertrophy can improve myocardial contractile function. The level of the functional-metabolic response in pygmy wood mice in the EURT area increased with increasing whole-body radiation dose rate and was more pronounced with a large pygmy wood mouse population size. The harmful effects (cardiac decompensation stage) of synergies resulting from non-radiation and radiation factors manifest after population abundance above 30 ind./100 trap-day and a radiation burden above 0.1 mGy/day.

1. Introduction

Since the beginning of the 21st century, in the field of radiation protection, the ecocentric principle of environmental protection against ionizing radiation has been discussed in view of the great variety of plants and animals that could be exposed to radiation considering the ever-growing anthropogenic pressure to biota (Pentreath, 2002). Much of the radiation effects data for non-human biota is from laboratory studies and there is a need for research into the consequences of exposure to radiation and the associated risks to populations of plants and animals from contaminated environments. This has been the approach advocated by the United Nations Scientific Committee on the Effects of Atomic Radiation (UNSCEAR, 2008), consistent with the International Commission on Radiological Protection (ICRP, 2008).

On September 29th, 1957, 74 PBq of radioactive wastes were released into the environment as a result of the accident at the Mayak Plant (Southern Urals, Russia). As a result, a vast territory (about 20,000 km^2) was contaminated. The radioactive contamination zone was called the East-Urals Radioactive Trace or EURT (UNSCEAR, 1993). In 1967, the same area was subjected to a secondary contamination resulting from the transport of radioactive sediments by the wind from the Mayak technological reservoir, Lake Karachay. Today, the main dose-forming radionuclides in the EURT zone are the β-emitters ^{90}Sr and its daughter ^{90}Y and the β/γ-emitter ^{137}Cs, with a specific activity in the soil two orders of magnitude lower than that of ^{90}Sr + ^{90}Y. Although many years have elapsed since the accident, the contemporary radiation situation remains elevated over the natural regional background and is mostly determined by long-lived ^{90}Sr that has been concentrated in the upper layers of the soil (Molchanova et al., 2014). The increased radionuclide contents in the environment pose a potential danger to the local biota.

In this paper, we present a study of functional-metabolic changes in the myocardium of pygmy wood mice inhabiting the EURT area. From the standpoint of classical radiobiology (Yarmonenko, 1984), cardiac muscle fibers are highly resistant to

* Corresponding author.
E-mail addresses: naorekhova@mail.ru (N.A. Orekhova), mmodorov@qmail.com (M.V. Modorov).

http://dx.doi.org/10.1016/j.jenvrad.2017.04.005
0265-931X/

radiation because of the low mitotic activity of cardiomyocytes (CMC). It is believed that most of the damaging effects on the myocardium are due to the effect of radiation on blood vessel endothelium, hemodynamic instability and increased of coronary vascular permeability, leading to damage at the structural and functional levels (Bandazhevskaya et al., 2004). These lethal effects are detected at radiation doses of 100 Gy or more in the mouse heart (Casarett, 1980). The decline in the respiratory activity of the myocardium and ultrastructural disorders can be attributed to the effects of ^{137}Cs that are considered from the perspective of the impact of the cesium ions as the radioactive element and potassium antagonist (Gritsuk et al., 2002; Kuznetsova et al., 2009). Parameters of mitochondrial oxidation and the ultrastructure of the myocardium in white rats were studied on a background of the consumption of food supplemented with ^{137}Cs at 60 or 600 Bq/kg (calculated doses were 1.5 and 15 μGy, respectively). Ultrastructural findings included swelling of mitochondria, matrix clarification, a partial reduction in the number of crists, and myelin-like bodies in the matrix. Considerable nucleus structural polymorphism was also observed with extension of the perinuclear space, spotted distribution of chromatin and modifications to the myofibril structure. These morphofunctional changes can be considered a reflection of apoptosis associated with the activation of peroxidation (Gritsuk et al., 2002). To a large extent, the changes in cardiomyocytes in animals from the radioactively contaminated areas resemble changes associated with the stress response and aging processes (Kudyasheva et al., 2004; Bulanova et al., 2008).

Given the fact that we are dealing with exposure to ionizing radiation in the environment, ecological factors may be able to modify radiation-induced biological effects (Kudyasheva et al., 2007; Petin and Jin Kyu Kim, 2014). For mouse-like rodents, a significant stress factor is high population abundance (Christian, 1963; Rogovin and Moshkin, 2007). In this context, the study of the patterns and the mechanisms of the radiation effect with the simultaneous influence of population overabundance is particularly important. This allows for an adequate estimation of the role of radiation and the determination of the permissible level of irradiation in a population with respect to the specific radioecological situation.

The aim of this study was to analyze, while taking into account population abundance and the whole-body radiation dose rate, the functional-metabolic changes in the myocardium of the pygmy wood mouse (*Apodemus uralensis* Pall., 1811) located in the EURT zone.

2. Materials and methods

Animal experiments were conducted at the Institute of Plant & Animal Ecology UB RAS (Russia) and approved by the local ethics committee.

2.1. Study locations and aims of the study

Samples from control (reference) plots and radionuclide contaminated (impact) plots were obtained in the course of trapping the pygmy wood mouse populations in the Southern Urals in July-October of 2010–2014. The impact study plots were located on the southwestern shore of Uruskul Lake (55°49′N, 60°53′E), 20 km from the epicenter of the accident at the Mayak plant (Fig. 1). The density of soil contamination with ^{90}Sr in that location is 3.3–22.3 MBq × m^{-2} (Atlas of the East Ural…, 2013). The reference (control) mice were caught in three areas located beyond the EURT zone, namely in Chelyabinsk Oblast (55°47′ N 61°22′ E) and Kurgan Oblast (54°22′ N, 64°29′ E; 54°47′ N, 66°27′ E). The level of soil contamination with ^{90}Sr in the reference regions was representative of the background in the Urals (0.3–3 kBq × m^{-2}) (Molchanova et al., 2014), and the ^{90}Sr specific activity in the bones of the reference mice was within the range of 0.2–0.6 Bq × g^{-1} (Starichenko et al., 2014).

Characterization of the trapping plots (periods of capture, relative abundance of mice, biotopic screening) is shown in Table 1. The pygmy wood mouse (*Apodemus uralensis* Pallas, 1811) is one of the most numerous species of small mammals inhabiting the anthropogenically transformed areas of the Ural region (wheat fields, forest plantations, fallow fields, gardens, areas transformed by chemical pollution, etc.) (Nurtdinova and Pyastolova, 2004; Mukhacheva et al., 2010). Similarly, on the ruderal meadow in the EURT area, this rodent is the most numerous of the small mammal fauna (Grigorkina et al., 2008). In the EURT area, pygmy wood mice can reach high numbers in birch groves if there are tier shrubs or dwarf shrubs (rose, cherry, raspberry) present. As controls, we used animals (reference mice) caught in similar habitats located in areas with a background level of radiation contamination.

In this study, immature mice aged 1–4 months and weighing more than 10 g were used. The age of mice was determined based on analysis of the generative and dental systems (Klevezal, 2007). A total of 113 individuals were collected from the radionuclide contaminated area and 70 individuals were collected from the control (reference) sites.

2.2. Trapping methods and the method of calculating the relative abundance of the pygmy wood mouse

Animals were trapped in accordance with generally accepted methods (Karaseva et al., 2008). Live-mouse traps with standard bait (bread and sunflower seed oil) for trapping rodents were used. The traps in groups of 10–25 units were placed in a line at a distance of 3–5 m from each other for a period of 2–10 days. The trap line length was restricted so that the line was located within a homogeneous plant association. Two days of trapping were enough to determine the relative abundance of animals.

The relative abundance was calculated using the formula:

$$N = (I/2 \times T) \times 100 \quad (1)$$

where N is the relative abundance of animals, I is the number of pygmy wood mice collected in the first two days after setting the traps and T is the number of traps in the line. Thus, the relative abundance for each line of traps was calculated and is represented as ind./100 trap-day.

Based on our own observations and the long-term monitoring of mouse-like rodent populations in the EURT zone (Grigorkina et al., 2008; Grigorkina and Olenev, 2013), an abundance of animals from 1 to 15 ind./100 trap-day was considered a small population size, from 15 to 30 ind./100 trap-day was a medium population size, and above 30 ind./100 trap-day was considered a large population size.

2.3. Methods of the biochemical studies

Animals were killed by fracturing the cervical vertebrae upon collection at the trap site. Within 15 min after death, the myocardium was weighed and frozen in liquid nitrogen. The biosamples were transported to the laboratory in a dewar, then stored in a freezer at a temperature of −80 °C until further biochemical analysis.

During our biochemical studies, we measured the concentrations of total lipids, protein and nucleic acids (DNA, RNA) and analyzed the activity of three enzymes, i.e. succinate dehydrogenase (SUCDH, EC 1.3.99.1), glucose-6-phosphate isomerase (GPI, EC 5.3.1.9) and catalase (CAT, EC 1.11.1.6). The level of lipid peroxidation

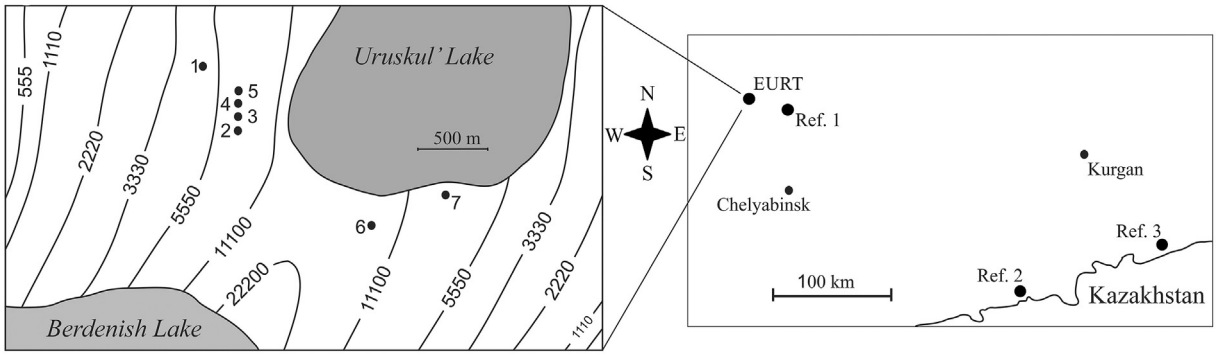

Fig. 1. Trap placement. Left - trapping plots on the territory of EURT. Isolines show territory with contamination density ^{90}Sr (kBq × m^{-2}) according to (Atlas of the East Ural..., 2013). Right - layout of the impact and reference areas. It shows the boundaries of the Russian Federation (RF) and Kazakhstan, and the location of the regional centers of the RF.

Table 1
Characterization of trapping plots: periods of capture, relative abundance of mice, biotopic screening.

Area	Plots of trapping	Year of trapping	Month of trapping	Relative abundance of mice, ind./100 trap −day	Sample size for biochemical analysis, n	Characteristics of the biotope in which the animals were caught
EURT	1	2012	July	12	7	Thin birch park type with a significant amount of decomposed litter. Animal captures were confined to the wild rose bushes.
	2	2011		38	23	Located approximately 500 m west of the lake on the site of the village, after the formation of EURT resettlement. With the help of earthmoving machinery, all buildings constructed here were destroyed and buried in specially dug trenches. The vegetation cover is represented by ruderal areas of the community, with most of the vegetation comprising bromus inermis (*Cirsiumsetosum* (Willd.) Bess.), nettle (*Urticadioica*L.), woolly thistle (*Bromopsisinermis* (Leyss.) and bluegrass (*Poa*sp.). There were 2–5 plots removed from each other by a distance of 100–300 m.
		2012		48	7	
		2014		2	1	
	3	2011		32	21	
		2012		30	16	
	4	2011		12	7	
		2012		50	3	
	5	2011		4	4	
		2012		10	2	
	6	2012		8	2	The vegetation cover is represented by ruderal areas of the community, with most of the vegetation comprising bromus inermis (*Cirsiumsetosum* (Willd.) Bess.) and woolly thistle (*Bromopsisinermis* (Leyss.).
	7	2012		26	15	Birch copse with an admixture of aspen, located at 100–300 m from the lake. Uruskul.
		2014		12	5	Animal captures are confined to the cherry bushes growing in the area.
Ref. 1	8	2010	October	11	11	Birch-aspen groves with wild rose growing among the meadows and reservoirs. The distance between the plots was 100–500 m.
	9	2010		28	17	
	10	2010		6	1	
	11	2010		17	3	
	12	2010		6	1	
Ref. 2	13	2011	August	2	1	Abuttal between an agrocenosises covered with weeds
	14	2012		24	4	Border of a meadow steppe and willow shrubs
	15	2012		7	4	Border of a wheatfield and meadow steppe
	16	2012		27	2	The ravine near a wheatfield.
	17	2012		65	12	Border of a mown hayfield and willow shrubs
Ref. 3	18	2011		21	12	Waterlogged birch-aspen-willow grove in the field
	19	2012		20	1	Steppe
	20	2012		4	1	Wheatfield

(LPO) was estimated on the basis of the concentration of secondary products of LPO reacting with thiobarbituric acid reactive substances (TBARS). We calculated mass ratios (total lipids/protein, DNA/total protein, total RNA/total protein, total RNA/DNA) as well as the relative mass fraction of nuclear, mitochondrial, cytoplasmic proteins.

The myocardium was homogenized in Tris-HCl buffer (0.025 mol/l, pH 7.4) containing 0.175 mol/l KCl. Nucleic acids (DNA, RNA) were extracted from tissue homogenates by alkaline (0.3 mol/l KOH) and acid (0.5 mol/l $HClO_4$) hydrolysis (Dell'Anno et al., 1998). The total lipids were extracted from the tissue homogenate with an ethanol:petroleum ether mixture (2:1).

The division into sub-cellular fractions (nuclear, mitochondrial and cytoplasmic) of tissue homogenate was carried out using the Schneider (1948) method. Spectrometric methods were used to estimate the concentrations of substances and enzyme activity. The lipid test was carried out using a vanillin solution (Fletcher, 1968), the protein test employed Coomassie Brilliant Blue G250 (Kruger, 2002), the TBARS test used thiobarbituric acid (Buege and Aust, 1978) and the nucleic acid (DNA, RNA) test employed diphenylamine (Dell'Anno et al., 1998). The enzyme activity was recorded using standard procedures with sodium succinate and 2,3,5-triphenyltetrazolium chloride for SUCDH (Kun and Abood, 1949), glucose-6-phosphate and resorcinol for GPI (Roe and Papadopoulos, 1954), and H_2O_2 and ammonium molybdate solution to assess CAT (Goth, 1991).

2.4. Determining ^{90}Sr and ^{137}Cs exposure of A. uralensis

In order to estimate the external exposure of animals to ^{137}Cs and ^{90}Sr, Tier 2 of the ERICA tool version 1.2.1 (Brown et al., 2008, 2016) was used. We adopted the following model parameters: a pygmy wood mouse, as a terrestrial mammal, lives 20% of the time on the ground, and 80% in the upper layer of the soil to a depth of

10 cm. The size of the animal is 2 × 2 × 8 cm. The specific activity of ^{90}Sr and ^{137}Cs in the soil layer 0–10 cm from the southern and western shores of Uruskul Lake was taken from the work of Molchanova et al. (2009). Plots 6 and 7 (see Fig. 1) were located on the southern shore of Uruskul Lake and plots 1–5 on the western shore. The analysis of these results is shown in Table 2.

The ^{90}Sr+^{90}Y specific activity in the jaw was obtained via non-destructive β-radiometry, as previously described (Malinovsky et al., 2012). When converting from the β-particle count rate in the jaw to the ^{90}Sr+^{90}Y specific activity, we used the formula:

$$y = 16 \times x^{0.78} + 3 \quad (2)$$

where y is the specific activity ^{90}Sr+^{90}Y in the jaw (Bq × g^{-1}) and x is the β-particle count rate, normalized to the wet weight of the jaw (impulse × s^{-1} × g^{-1}).

These results have previously been reported in detail (Starichenko and Modorov, 2013) but, in summary, it was decided that the ^{90}Sr+^{90}Y specific activity in the skeleton of a pygmy wood mouse from the EURT area is 78% of the specific activity in the jaw, and the ^{90}Sr specific activity is half of the total value obtained. The conversion coefficient linking the skeleton ^{90}Sr activity concentration and the whole-body dose rate received during 1 day is 1.5 × 10^{-6} (mGy/day)/(Bq/kg of skeleton weight) (Malinovsky et al., 2014).

In the calculation of internal doses from ^{137}Cs, it was accepted that the geometric average rate of transition to terrestrial herbivorous mammals is 1.5 (IAEA, 2014). The animal internal unweighted radiation dose for a given specific activity of ^{137}Cs in the soil is equal to 0.005 mGy/day for plots 1–5 and for 0.030 mGy/day plots 6 and 7.

2.5. The statistical analysis of the data

The calculations were performed using STATISTICA version 8.0 and STATGRAPHICS version 8.0 software. Mathematical processing of the data was performed by the analysis of covariance (ANCOVA), regression analysis and the Mann-Whitney *U* test (StatSoft, 2012).

The effect of the gender factor on the variability of biochemical indicators was assessed by the Mann-Whitney *U* test by comparing parameters in males and females trapped at one particular plot. The six trapping plots (plots 9, 7, 3, 2, 17, and 18) used for this comparison were balanced with respect to sexual composition. A significant difference between males and females was not found (Appendix 1). Therefore, it was decided to combine males and females into a single group.

The abundance of *A. uralensis* in the Ref. 1 area varied from 6 to 28 ind./100 trap-day, from 2 to 65 ind./100 trap-day in the Ref. 2 area, and from 4 to 21 ind./100 trap-day in the Ref. 3 area. To justify the unification of reference mice from geographically remote trapping plots, a comparison of Ref. 1, Ref. 2 and Ref. 3 was carried out by ANCOVA (Appendix 2). We used the homogeneity-of-slopes model to test whether a continuous predictor (abundance of mice, ind./100 trap-day) has different effects at different levels of a categorical factor (Ref. 1/Ref. 2/Ref. 3). The interaction effect of categorical and continuous predictors was not statistically significant at $p \leq 0.05$. No biochemical differences were evident between Ref. 1, Ref. 2 and Ref. 3. Therefore, it was decided to combine the reference mice into a single group.

The abundance of mice varied from 2 to 50 ind./100 trap-day in the EURT zone, and from 2 to 65 ind./100 trap-day in the reference areas. The dependence of the analyzed biochemical parameters on the relative abundance of animals was described by a linear regression equation: $y = b_0 \pm b_1 \times x$. For all equations, the 95% confidence limits for b_1 coefficient values, obtained for the study and reference samples, did not overlap, and the absolute values of the b_1 coefficient in the samples from the contaminated area were always higher (Appendix 3). To take into account the interaction of categorical (reference/impact) and continuous (abundance of mice, ind./100 trap-day) predictors, ANCOVA was used on the basis of the separate-slopes model.

3. Results

The ANCOVA results on the basis of the separate-slopes model are presented in Fig. 2 and Table 3. At this stage, we ignored differences in the radiation dose rate at the impact sites.

The myocardium of *A. uralensis* from the EURT area demonstrated an increase in the concentrations of protein, total lipids, TBARS, RNA and DNA, as well as higher GPI activity, whereas the levels of CAT and SUCDH activity were reduced. In addition, a distinct increase in the RNA concentration, as compared with changes in the DNA and protein concentrations, led to an increase in the RNA/protein and RNA/DNA ratios. The same was observed in the mass ratios in the myocardium of *A. uralensis* within the EURT area, where an increase in total lipids/protein and DNA/total protein was found.

The interaction effect of categorical (reference/impact) and continuous (abundance of mice) predictors was statistically significant at $p \leq 0.05$. Because of this, with a small population size (10 ind./100 trap-day), the level of biochemical shifts in the study sample ranged from 1% to 36% relative to the reference values, whereas those from a medium-sized population (20 ind./100 trap-day) ranged from 10% to 54%. For large population sizes, the changes with respect to the reference group of animals were characterized as 15–69% for 30 ind./100 trap-day, 21–88% for 40 ind./100 trap-day and 106–263% for 50 ind./100 trap-day.

The effect of the unweighted whole-body total (i.e. internal and external) radiation dose rate assessed for ^{90}Sr and ^{137}Cs on the biochemical parameters of the impact animals is shown in Fig. 3. The figure shows that the description of dependence by a linear equation is only possible if one ranks the study sample into two groups according to the population size: from 2 to 26 ind./100 trap-day *(a)* and from 30 to 50 ind./100 trap-day *(b)*. Group *b* included mostly individuals trapped on plots 2 and 3, whereas in group *a*, individuals were from plots 1, 4, 5, 6 and 7.

According to the regression analysis (Table 4), the 95% confidence limits for the b_1 coefficient values obtained for the two

Table 2
Radiation burden caused by ^{90}Sr and ^{137}Cs in animals trapped within the EURT zone.

Plots	Specific activity of a radionuclide in the soil layer 0–10 cm[a]				External dose rate	
	^{90}Sr		^{137}Cs		^{90}Sr	^{137}Cs
	Bq × kg^{-1}	kBq × m^{-2}	Bq × kg^{-1}	kBq × m^{-2}	mGy/day	
1–5	35,537	610	958	27	1.06 × 10^{-7}	0.006
6,7	98,210	2780	5571	102	2.90 × 10^{-7}	0.035

[a] Data are from Molchanova et al. (2009).

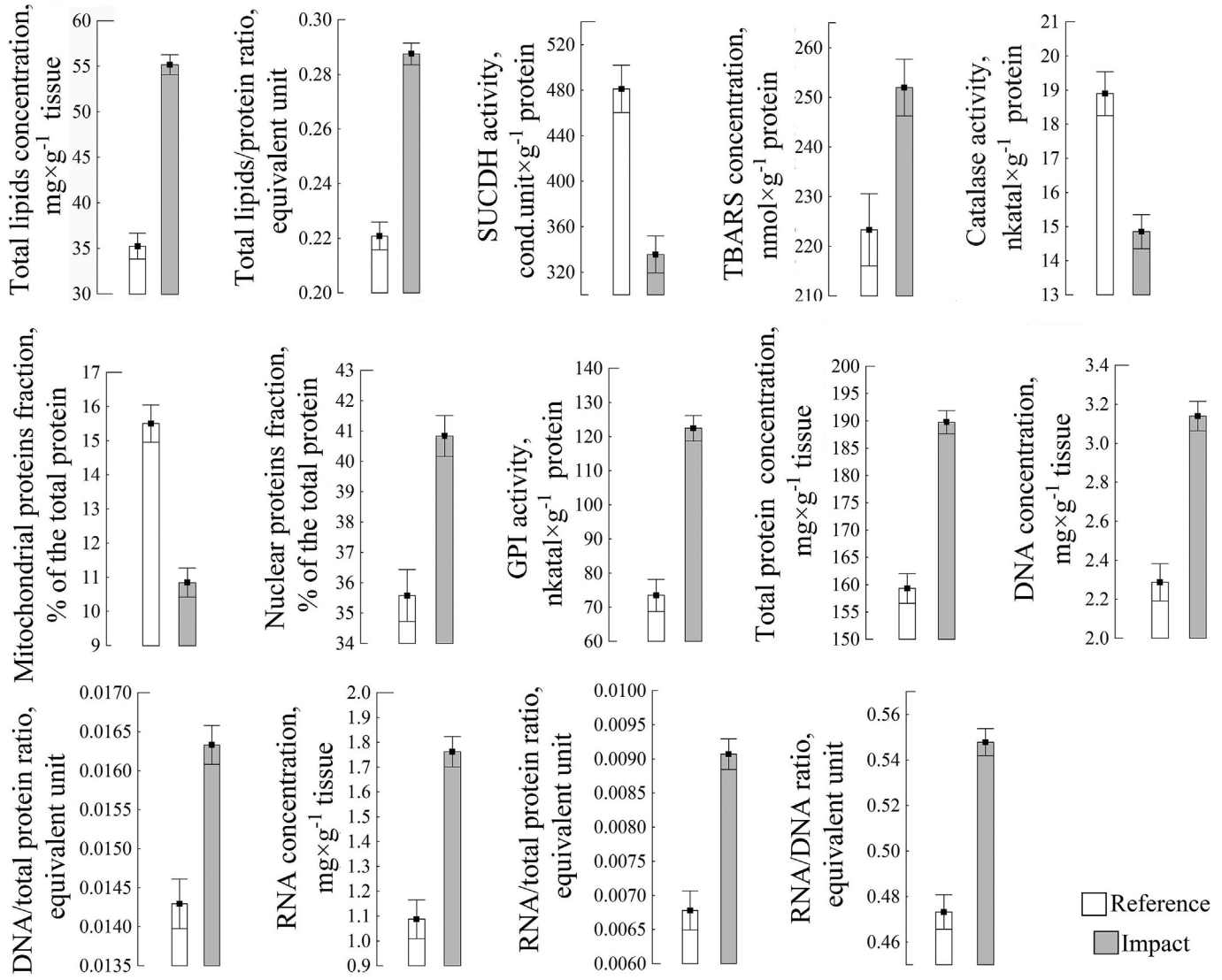

Fig. 2. Biochemical parameters of the myocardium for *A. uralensis* trapped in the control territory (reference) and within the EURT zone (impact) at population abundance equal to 27 ind./100 trap-day computed for covariates at their means; the results of ANCOVA on the basis of the separate-slopes model.
Bars – average mean; whiskers – 95% confidence limit for average mean.

groups do not overlap, while the values of the b_1 coefficient were higher in group *(b)*. Thus, the results demonstrate dose-dependent functional-metabolic effects in the myocardium of *A. uralensis* in the EURT area. These changes were more pronounced in large populations.

4. Discussion

4.1. Changes in the biochemical parameters in A. uralensis within the EURT area: description of functional-metabolic myocardial effects

The total lipid concentration and lipid/protein ratio. An increase in the lipid concentration and the lipid/protein concentration ratio in the tissue of mice from the EURT area was observed. This situation may arise if there is an increase in the fatty free acid concentration in cells, which are not part of the lipoprotein complexes of intracellular structures and accumulate in cytoplasmic lipid droplets. In the case of the normal cardiac physiology, lipids do not accumulate because they are spent continuously on the synthesis of macroergic compounds. In general, lipids provide more than 70% of the energy required for the contractile activity of myocardial cells (Weiss et al., 1989). The reason for the "redundancy" of labile fats is due to limited catabolism and their limited participation in the energy supply of the CMC.

SUCDH activity. Because of the limited participation of lipid catabolism products (acetyl-ScoA) in the tricarboxylic acid cycle (TCA cycle), the SUCDH activity decreased. Taking into account the fact that SUCDH is located on the inner mitochondrial membrane, the decrease in the SUCDH activity may also be associated with the reduced mitochondrial density in the CMC. Accumulating fatty acyls, which are not used in metabolic cycles, can act as a detergent on the mitochondrial membrane (Skulachev, 1989). Since 90% of adenosine triphosphate (ATP) in a normal heart is produced by mitochondrial oxidative metabolism (Harris and Das, 1991), the observed decrease in lipid catabolism and activity of a key enzyme of the TCA cycle will control the state of the energy deficit in the myocardium of mice from the EURT area.

Table 3
Univariate tests of significant differences for the biochemical parameters of *A. uralensis* trapped in the reference area and the EURT: the results of ANCOVA on the basis of the separate-slopes model.

Parameter	(R^2)[a]	SS[b]			*F* (1.12)		*p*		Percentage changes of biochemical parameters of the EURT area[c]				
		SS_{B1}	SS_{B2}	SS_R	F_{B1}	F_{B2}	p_{B1}	p_{B2}	Population abundance, ind./100 trap−day				
									10	20	30	40	50
Total lipids concentration	0.83	14087.98	5.96	6413.88	197.7	0.2	$<10^{-6}$	0.683	**+22**	**+41**	**+56**	**+78**	**+92**
Total lipids/protein ratio	0.80	0.124536	0.000002	0.081826	136.9	0.0	$<10^{-6}$	0.948	**+11**	**+22**	**+32**	**+43**	**+52**
SUCDH activity	0.76	3423036	46944	1401886	219.7	6.0	$<10^{-6}$	0.015	−2	**−15**	**−34**	**−57**	**−87**
TBARS concentration	0.47	113819	4626	170519	60.1	4.6	$<10^{-6}$	0.028	**+12**	**+13**	**+13**	**+13**	**+13**
Catalase activity	0.69	2240.33	5.99	1336.23	150.8	0.8	$<10^{-6}$	0.370	−1	**−12**	**−24**	**−33**	**−47**
Sub-cellular fractions:	0.67	3548.98	0.98	2383.55	134.0	0.0	$<10^{-6}$	0.785	+5	**+11**	**+16**	**+20**	**+24**
nuclear	0.75	1945.64	36.77	961.42	182.1	6.9	$<10^{-6}$	0.009	**−16**	**−23**	**−32**	**−44**	**−59**
mitochondrial													
GPI activity	0.73	89996.4	431.7	72396.4	111.8	1.1	$<10^{-6}$	0.301	**+36**	**+54**	**+69**	**+82**	**+94**
Total protein concentration	0.77	38323.4	163.0	23773.8	144.5	1.2	$<10^{-6}$	0.268	+1	**+15**	**+21**	**+25**	**+30**
DNA concentration	0.74	47.6588	0.0836	29.3376	146.2	0.5	$<10^{-6}$	0.474	+12	**+27**	**+40**	**+51**	**+61**
DNA/total protein ratio	0.65	0.000415	0.000002	0.000329	113.6	1.0	$<10^{-6}$	0.305	+3	**+10**	**+15**	**+21**	**+26**
RNA concentration	0.72	30.11706	0.39569	19.6656	137.8	3.6	$<10^{-6}$	0.058	+13	**+43**	**+67**	**+88**	**+106**
RNA/total protein ratio	0.71	0.000408	0.000007	0.000267	137.4	4.4	$<10^{-6}$	0.032	+5	**+22**	**+37**	**+51**	**+63**
RNA/DNA ratio	0.76	0.326520	0.005688	0.185889	158.0	5.5	$<10^{-6}$	0.020	+2	**+10**	**+17**	**+25**	**+31**

Bold font — biochemical changes from the EURT area are statistically significant at $p = 0.05$.
[a] The determination coefficient (1- SS_R/SS_t) of the ANCOVA.
[b] The sum of squares on account: SS_{B1} — interaction effect of categorical (reference/impact) and continuous (population abundance) predictors; SS_{B2} — effect of categorical predictor; SS_R —errors of prediction.
[c] $\frac{(M_{EURT}-M_{reference})}{M_{reference}} \times 100\%$, where M is average value.

TBARS concentration and CAT activity. Despite the reduction in aerobic ATP synthesis, a part of the LPO induction process (Lenaz, 1998), the TBARS concentration did not decrease and even had a tendency to exceed the reference level. A reduction in antioxidant (AO) protection (in particular, CAT activity) is also a factor that contributes to an increase in LPO products. It plays a leading role in protecting cells and subcellular structures from the toxic effects of H_2O_2 (Eaton, 1991). The buffer capacity of the AO system in a radioactively contaminated environment is probably not sufficient to support the process of LPO at the control level. As a consequence, we observed the preconditions for a progressive imbalance in the LPO-AO system and the development of free radical damage to the CMC as well as structural and functional abnormalities in mitochondria. Significantly, lower antioxidant concentrations (retinol, α-tocopherol and carotenoids) have been observed in blood plasma, liver and egg yolk of birds inhabiting areas contaminated by Chernobyl (Møller et al., 2005) —an effect attributed to radiation-induced oxidative stress. However, the relationship between antioxidant concentrations and oxidative stress is complex. There is study that not supports the hypothesis that direct oxidizing stress is a mechanism for damage to organisms exposed to chronic radiation at dose rates typical of contaminated environments (Smith et al., 2012).

GPI activity was increased in mice from the EURT area. This is evidence of the increasing role of carbohydrates in energy metabolism. It is probable that this increase has a compensatory function and is associated with a decrease in lipid catabolism. The increase in the GPI activity against the background level of the SDG activity was lower than in the reference group. This indicates that the aerobic oxidation of glucose in the TCA cycle was limited, and the anaerobic degradation of glucose contributes to the energy supply system of the myocardium. A similar pattern was revealed previously in an analysis of bioenergetic processes in the myocardium of voles inhabiting ecosystems with high levels of natural radioactivity (Kudyasheva et al., 2004). Despite the low efficiency of anaerobic glycolysis in the generation of macroergic compounds (only two molecules of ATP, while the aerobic oxidation of glucose produces 38 molecules of ATP), this metabolic cycle plays a leading role in the mechanisms of the myocardial response to the effects of external (abiotic and biotic) and internal stress factors (Meyerson, 1981).This is due to the fact that glycolysis at all stages of the reaction of glucose 6-phosphate (GLP) → phosphoglycerate could be a source of initial substrates for the synthesis of nucleotides and proteins (Guppy et al., 1993) and, as a result, contributes to the development of compensatory hypertrophy that improves myocardial contractile function under conditions of low energy shift. Taking this into consideration, it can be assumed that GPI activation in the myocardium of mice from the EURT area is a precondition for the observed increase in protein and DNA concentrations in metabolic tissue.

DNA, protein concentrations and the DNA/protein ratio. Myocardial hypertrophy in mammals can be caused by cell division (proliferation) and an increase in the size of CMC due to polyploidy and/or an increase in the volume of cytoplasmic structures (Shpońka, 1996). The protein and DNA concentrations in the myocardium of animals from the EURT area increased due to the higher number of cells per unit mass of tissue. An increase in the DNA/protein concentration ratio, which characterizes the development of CMC ploidy (Anatskaya and Vinogradov, 2004), was observed in impact samples. It is assumed that cells with excess genome have a large reserve for the subsequent growth of the cytoplasm and consequently have an advantage under physiological and pathological stress conditions (Brodskiy et al., 1985). The influence of polyploidy is also manifested in the increase of the expression level of *HIF-1α*, which helps to maintain the contractile function of CMC with reduced aerobic capacity (Haddad et al., 2006; Secades et al., 2009).

RNA concentration, RNA/protein and RNA/DNA ratios. A distinct increase in the RNA concentration, as compared with changes in the DNA and protein concentrations, led to an increase in the RNA/protein and RNA/DNA ratios. This indicates a higher density of RNA molecules per unit mass of protein and DNA, which allows us to suggest a high intensity of development of the protein-synthesizing system in CMC in mammals from the EURT area.

In this way, the complex of revealed changes in the biochemical parameters of *A. uralensis* from a radioactive contaminated area allows us to assume the development of compensatory myocardial

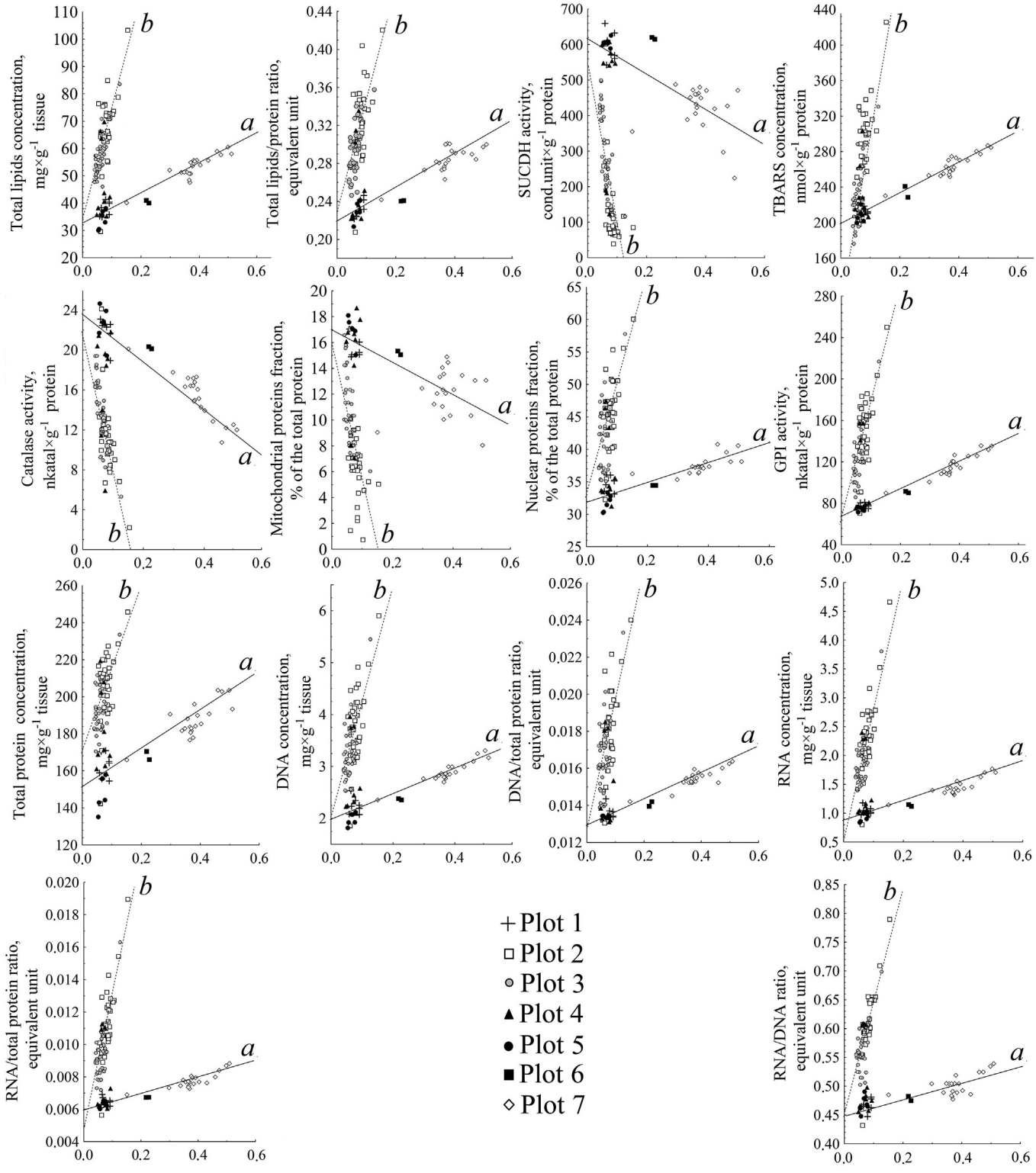

Fig. 3. Effect of the whole-body radiation dose rate on biochemical parameters in *A. uralensis* within the EURT area in two groups according to the population abundance: from 2 to 26 ind./100 trap-day *(a)* and from 30 to 50 ind./100 trap-day *(b)*.
X-axis: values of the unweighted total (i.e. internal and external) radiation dose rate, mGy/day.

hypertrophy due to increased cell numbers, CMC ploidy and protein synthesizing activity. Compensatory myocardial hypertrophy can improve the contractile function of the organ due to the low efficiency of cell energy production. A possible scheme of the process is shown in Fig. 4.

4.2. Dose-dependent functional-metabolic effects: modification of the curve taking into account the population abundance

The functional-metabolic myocardial response to the radiation burden was modified by the factor “relative abundance of mice”

Table 4
Effect of whole-body radiation dose rate (x_1) and abundance of mice (x_2) on the biochemical parameters (y) in *A. uralensis* within the EURT area in two groups according to the population size (moderate, large): the results of multiple linear regression $y = b_0 \pm b_1 \times x_1 \pm b_2 \times x_2$.

Parameter	Population size									
	moderate (from 2 to 26 ind./100 trap–day)					large (from 30 to 50 ind./100 trap–day)				
	df(n-2) = 41					df(n-2) = 68				
	$b_0 \pm$ SE	$b_1 \pm$ SE*	β_1	$b_2 \pm$ SE*	β_2	$b_0 \pm$ SE	$b_1 \pm$ SE*	β_1	$b_2 \pm$ SE*	β_2
Total lipids concentration	**31.1 ± 0.9**	**46.4 ± 3.6**	0.82	**(20.1 ± 7.2) × 10^{-2}**	0.18	**16.5 ± 3.7**	**305.3 ± 32.2**	0.61	**(72.1 ± 10.9) × 10^{-2}**	0.42
Total lipids/protein ratio	**(21.3 ± 0.3) × 10^{-2}**	**(15.2 ± 1.2) × 10^{-2}**	0.84	**(5.5 ± 2.5) × 10^{-4}**	0.15	**(17.2 ± 1.6) × 10^{-2}**	**(92.3 ± 14.1) × 10^{-2}**	0.55	**(21.3 ± 4.8) × 10^{-4}**	0.37
SUCDH activity	**663.1 ± 17.1**	**341.8 ± 65.9**	−0.55	**4.8 ± 1.3**	−0.39	**686.3 ± 58.8**	**4041.4 ± 506.3**	−0.65	**5.1 ± 1.7**	−0.24
TBARS concentration	**197.1 ± 2.3**	**162.5 ± 8.9**	0.92	0.2 ± 0.2	0.07	**99.2 ± 21.1**	**1624.1 ± 181.5**	0.71	**1.4 ± 0.6**	0.17
Catalase activity	**23.6 ± 0.5**	**21.0 ± 1.9**	−0.89	(18.9 ± 38.0) × 10^{-3}	−0.04	**23.3 ± 1.5**	**126.2 ± 13.3**	−0.75	(58.0 ± 45.3) × 10^{-3}	−0.10
Sub-cellular fractions:	**31.9 ± 0.4**	**12.1 ± 1.8**	0.71	**(0.6 ± 0.3) × 10^{-1}**	0.21	**27.8 ± 2.9**	**137.2 ± 25.6**	0.53	**(2.1 ± 0.8) × 10^{-1}**	0.24
nuclear	**18.5 ± 0.4**	**6.5 ± 1.8**	−0.38	**(1.8 ± 0.3) × 10^{-1}**	−0.56	**18.5 ± 1.8**	**96.0 ± 15.5**	−0.59	(1.0 ± 0.5) × 10^{-1}	−0.18
mitochondrial	67.0 ± 1.3	**132.5 ± 5.0**	0.99	(54.6 ± 99.5) × 10^{-3}	0.02	20.8 ± 13.9	**994.8 ± 120.5**	0.65	**1.4 ± 0.4**	0.26
GPI activity	**148.1 ± 2.8**	**73.6 ± 10.6**	0.70	**0.5 ± 0.2**	0.25	**143.8 ± 7.9**	**343.3 ± 68.4**	0.47	**0.9 ± 0.2**	0.37
Total protein concentration										
DNA concentration	**1.9 ± 0.05**	**2.1 ± 0.2**	0.82	**(8.4 ± 3.7) × 10^{-3}**	0.17	**0.9 ± 0.3**	**19.1 ± 2.7**	0.32	**(35.0 ± 9.2) × 10^{-3}**	−0.49
DNA/total protein ratio	**(13.0 ± 0.1) × 10^{-3}**	**(55.5 ± 5.7) × 10^{-4}**	0.85	(12.0 ± 11.0) × 10^{-6}	0.09	**(9.9 ± 1.1) × 10^{-3}**	**(591.2 ± 93.8) × 10^{-4}**	0.57	**(98.0 ± 32.0) × 10^{-6}**	0.28
RNA concentration	**0.8 ± 0.03**	**1.3 ± 0.1**	0.85	(3.8 ± 2.2) × 10^{-3}	0.12	0.1 ± 0.2	**19.8 ± 1.8**	0.72	**(24.1 ± 6.3) × 10^{-3}**	0.26
RNA/total protein ratio	**(5.9 ± 0.9) × 10^{-3}**	**(43.8 ± 3.8) × 10^{-4}**	0.88	(7.0 ± 8.0) × 10^{-6}	0.07	**(2.5 ± 0.7) × 10^{-3}**	**(731.9 ± 66.6) × 10^{-4}**	0.74	**(77.0 ± 23.0) × 10^{-6}**	0.23
Total RNA/DNA ratio	**(45.7 ± 0.5) × 10^{-2}**	**(10.9 ± 0.2) × 10^{-2}**	0.84	**(1.7 ± 3.7) × 10^{-4}**	0.08	**(41.1 ± 1.8) × 10^{-2}**	**(18.6 ± 1.7) × 10^{-2}**	0.78	**(13.0 ± 5.5) × 10^{-4}**	0.16

β (beta) — standardized regression coefficient. df— degrees *of* freedom. * — the values of the regression coefficients are given by modulus.
Bold font — t-values for regression coefficient ≥ critical $t_{0.05}$ -value.

(Fig. 3; Table 4). The dose effects in the myocardium were more pronounced with a large population size (from 30 to 50 ind./100 trap-day) than the functional-metabolic changes observed in the impact group of rodents trapped at a lower (in 2.5 times) population size. This raises the question of how much chronic radiation exposure would have a negative effect on an organism living in an area with a large population. In this case, increased competition between individuals for environmental resources occurred, and, as a consequence, the stress response level increased. The animal's population therefore simultaneously incurred the powerful influence of radioactive and non-radioactive stressors.

In an ICRP publication (ICRP, 2008) on the radiation safety of biota, the ICRP introduced the concept of Reference Animals and Plants. Based on data on the biological effects of radiation for each reference organism, the Derived Consideration Reference Levels (DCRLs) have been defined. For existing or planned exposures, the doses to reference organisms are to be compared with relevant DCRLs. For the purposes of environmental protection, the ICRP recommends the representative organism, which is the actual object of protection under consideration. Each DCRL is regarded as a range of dose rates at which there is a possibility of harmful influences of ionizing radiation on representatives of this type of reference animal or plant. Murine rodents can be used as a representative organism for the EURT. The closest reference organism to these animals is the reference rat, for which the DCRL is 0.1–1 mGy/day.

In group *b* (from 30 to 50 ind./100 trap-day), even the 92nd percentile of the unweighted whole-body total (i.e. internal and external) radiation dose rate conducted for ^{90}Sr and ^{137}Cs was below the DCRL (the 25–75th percentiles is 0.056–0.083 mGy/day, with a median of 0.068 mGy/day, mean of 0.070 mGy/day and maximum value of 0.154 mGy/day). In group *a* (from 2 to 26 ind./100 trap-day) the median value of the dose (0.151 mGy/day) exceeded the lower boundary of the DCRL, in which the 25–75th percentile is 0.073–0.370 mGy/day. On the basis of multiple regression equations (Table 4), the stress response at a large population (over 30 ind./100 trap-day) can be compared when a moderate population size (group *a*: from 2 to 26 ind./100 trap-day) to stress during the simultaneous action of high abundance of mice and the radiation burden. At a population size of 32 ind./100 trap-day (the median value) and a dose rate of 0.068 mGy/day, the response was similar to that in an individual from group *a* with a small population size (10 ind./100 trap-day) with a radiation burden of 0.3–1 mGy/day, which exceeded the DCRL for three of the nine biochemical parameters. The value of 0.1 mGy/day for mice trapped at a population level of 30 ind./100 trap-day is equivalent to a radiation burden of 0.7–1.5 mGy/day. With a population level of 40 ind./100 trap-day, it is also equivalent to a radiation burden of 0.8–1.6 mGy/day, and at 50 ind./100 trap-day, a dose of 0.1 mGy/day is equivalent to a radiation burden of 0.8–1.7 mGy/day. Thus, the functional-metabolic effects caused by a radiation burden of 0.1 mGy/day are amplified by approximately ten-fold with the simultaneous action of a large population (over 30 ind./100 trap-day) as an environmental stressor. When there is a large population size, within the ICRP concept of a radiological protection system (ICRP, 2008), the optimization of protection of EURT biota should be aimed at reducing exposure to levels that are below the lower boundary of DCRL (less than 0.1 mGy/day). Otherwise, we should expect the possibility of harmful effects of synergies resulting from non-radiation and radiation factors, leading to a transition from adaptation to the stage of cardiac decompensation. In particular, the low activity of SUCDH and CAT and the mitochondrial protein content in the myocardium of a pygmy wood mouse living in an area with a large population are projected to be close to zero when the radiation burden is above

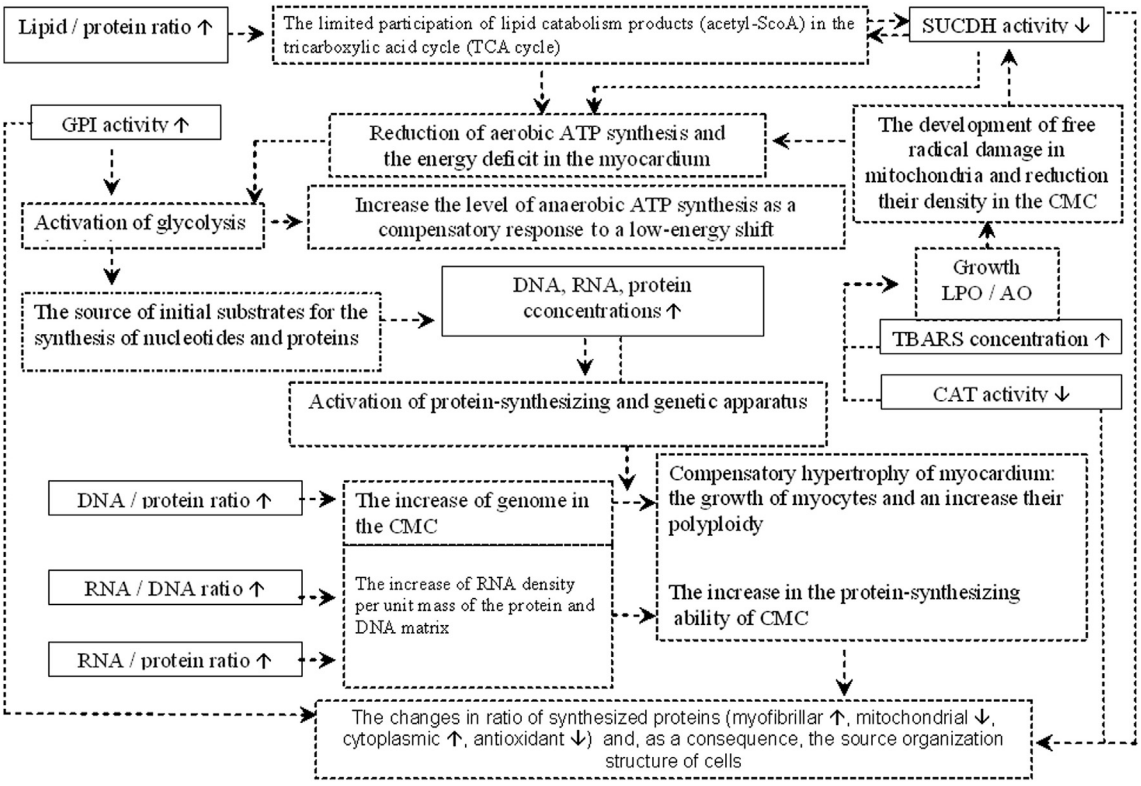

Fig. 4. The functional-metabolic myocardial effects in *A. uralensis* from the EURT area (probable scheme of the process).
Solid line – changes in biochemical parameters; dashed line – functional-metabolic parameters.

0.1 mGy/day. As a result of hypertrophy, the concentrations of glycolytic enzymes (in particular, GPI) and cytoplasmic proteins (in particular, contractile proteins) are increased predominantly. The decline in the mitochondria/myofibril ratio as well as hyperploidy can take place at increasing pathological loads in the stage of decompensation (Meyerson, 1981; Nepomnyashchikh, 1991; Lushnikova et al., 1994; Yu and Zhang, 1996).

5. Conclusion

The complex changes in biochemical parameters of *A. uralensis* from the EURT area with external and internal exposure to ^{137}Cs and ^{90}Sr (unweighted total dose rate 0.04–0.5 mGy/day) allowed us to assess the development of compensatory myocardial hypertrophy. Reduced lipid metabolism in the process of energy generation in cardiomyocytes, the excessive accumulation of labile fat, the decrease in the levels of mitochondrial oxidation and antioxidant protection, and the induction of lipid peroxidation are evidence of an energy deficit in the myocardium and the development of functional defects. The mechanisms counteracting these defects are compensatory activation of the anaerobic glycolytic system, an increase in cell numbers and cardiomyocyte hypertrophy due to genome ploidy and the capacity of the protein synthesizing apparatus.

The functional-metabolic effect caused by a radiation burden is amplified by the simultaneous action of population overabundance as an environmental stressor. The harmful effect (cardiac decompensation stage) of synergies resulting from non-radiation and radiation factors can manifest itself at a population abundance above 30 ind./100 trap-day and a radiation burden that exceeds the lower boundary of DCRL (above 0.1 mGy/day).

Funding

This work was supported by the Program for Basic Research, UB of RAS (Project № 15-2-4-21), and also by the Russian Foundation for Basic Research (project no. 14_04_01484_a).

Appendix A. Supplementary data

Supplementary data related to this article can be found at http://dx.doi.org/10.1016/j.jenvrad.2017.04.005.

References

Anatskaya, O.V., Vinogradov, A.E., 2004. Paradoxical relationship between protein content and nucleolar activity in mammalian cardiomyocytes. Genome 47, 565–578.
Atlas of the East Ural and Karachay Radioactive Trace Including Forecast up to 2047, 2013. IGCE Roshydromet and RAS, «Infosphere» Foundation, Moscow (in Russian). http://downloads.igce.ru/publications/Atlas/CD_VURS/index.html.
Bandazhevskaya, G.S., Nesterenko, V.B., Babenko, V.I., Yerkovich, T.V., Bandazhevsky, Y.I., 2004. Relationship between caesium (137Cs) load, cardiovascular symptoms, and source of food in 'Chernobyl' children—preliminary observations after intake of oral apple pectin. Swiss Med. Wkly. 134, 725–729.
Brodsky, V.Y., Delone, G.V., Tsirekidze, N.N., 1985. Genome multiplication in cardiomyocytes of fast- and slow-growing mice. Cell Differ. 17, 175–181.
Brown, J.E., Alfonso, B., Avila, R., Beresford, N.A., Copplestone, D., Pröhl, G., Ulanovsky, A., 2008. The ERICA tool. J. Environ. Radioact. 99, 1371–1383.
Brown, J.E., Alfonso, B., Avila, R., Beresford, N.A., Copplestone, D., Hosseini, A., 2016. A new version of the ERICA tool to facilitate impact assessments of radioactivity on wild plants and animals. J. Environ. Radioact. 153, 141–148.
Buege, J., Aust, S., 1978. Microsomal lipid peroxidation. In: Methods in Enzymology, vol. 52. Academic Press, New York.
Bulanova, K., Lobanok, L., Konoplya, E., 2008. Radiation and Chernobyl: Cardiomyocytes and Regulation of Their Functions. RNUP "Institut radiologii", Gomeĺ (in Russian).
Casarett, C., 1980. Radiation Histopathology. Boca Raton CRC Press, Florida.
Christian, J., 1963. Endocrine adaptive mechanisms and the physiologic regulation growth. Physiol. Mammal. 1, 189–353.

Dell'Anno, A., Fabiano, M., Duineveld, G., Kok, A., Danovaro, R., 1998. Nucleic acid (DNA, RNA) quantification and RNA/DNA ratio determination in marine sediments: comparison of spectrophotometric, fluorometric, and high performance liquid chromatography methods and estimation of detrital DNA. Appl. Environ. Microbiol. 64 (9), 3238–3245.
Eaton, J., 1991. Catalases and peroxidases and glutathione and hydrogen peroxide: mysteries of the bestiary. J. Laboratory Clin. Med. 118 (1), 3–4.
Fletcher, M., 1968. A colorimetric method for estimating serum triglycerides. Clin. Chim. Acta 22 (3), 393–397.
Grigorkina, E., Olenev, G., 2013. Radioecological researches of small mammals within the Eastern Urals Radioactive Trace: some outcomes. Radiat. Saf. Probl. Spec. Issue 14–24 (in Russian with English Abstract).
Grigorkina, E., Olenev, G., Modorov, M., 2008. Analysis of rodent populations in technogenically transformed areas (with reference to *Apodemus* (*S.*) *uralensis* from the EURT zone). Russ. J. Ecol. 39 (4), 284–291.
Gritsuk, A., Matyukhina, T., Koval, A., Gritsuk, N., 2002. Mitochondrial oxidation and ultrastructure of the myocardium on a background of incorporation of cesium radionuclides. Aviakosmicheskaya i Ekol. Meditsina 36 (2), 40–44 (in Russian with English Abstract).
Guppy, M., Greiner, E., Brand, K., 1993. The role of the Crabtree effect and an endogenous fuel in the energy metabolism of resting and proliferating thymocytes. Eur. J. Biochem. 212 (1), 95–99.
Goth, L., 1991. A simple method for determination of serum catalase activity and revision of reference range. Clin. Chim. ACTA 196, 143–152.
Haddad, F., Qin, A.X., Bodell, P.W., Zhang, L.Y., Guo, H., Giger, J.M., Baldwin, K.M., 2006. Regulation of antisense RNA expression during cardiac MHC gene switching in response to pressure overload. Amer. J. Physiol. Heart Circ. Physiol. 290, 2351–2361.
Harris, D., Das, A., 1991. Control of mitochondrial ATP synthesis in the heart. Biochem. J. 280, 561–560.
IAEA, 2014. Handbook of Parameter Values for the Prediction of Radionuclide Transfer to Wildlife. Technical Reports Series. International Atomic Energy Agency, Vienna.
ICRP, 2008. Environmental Protection: the Concept and Use of Reference Animals and Plants. ICRP Publication 108. In: Ann. ICRP, vol. 38. International Commission on Radiological Protection. Elsevier, Oxford, pp. 4–6.
Karaseva, E.V., Telitsina, A.Yu., Zhigalsky, O.A., 2008. The Methods of Studying Rodents in the Wild Nature. LKI, Moscow (in Russian).
Klevezal, G., 2007. Principles and Methods of Age Determination in Mammals. KMK, Moscow (in Russian).
Kruger, N., 2002. The Bradford method for protein quantitation. In: The Protein Protocols Handbook. Humana Press, pp. 15–21.
Kudyasheva, A., Shishkina, L., Shevchenko, O., Bashlykova, L., Zagorskaya, N., 2004. Biological Effects of Radioactive Contamination to Populations of Mose-like Rodents. Izdatel'stvo Ural'skogo Otdeleniya Rossiiskoi Akademii Nauk, Ekaterinburg (in Russian).
Kudyasheva, A., Shevchenko, O., Bashlykova, L., Zagorskaya, N., Shishkina, L., 2007. Biological consequences of increased natural radiation background for *Microtus oeconomus* Pall. populations. J. Environ. Radioact. 97 (1), 30–41.
Kun, E., Abood, L., 1949. Colorimetric estimation of succinic dehydrogenase by tryphenyl tetrazoliumchloride. Science 109 (2824), 144–146.
Kuznetsova, T., Maltsev, N., Tumanov, E., 2009. The compensatory adaptive response to myocardial incorporated radionuclides and hypokinesia. Morfologiya 135 (5), 46–49 (in Russian).
Lenaz, G., 1998. Role of mitochondria in oxidative stress and aging. Biochim. Biophys. Acta 1366 (1–2), 53–67.
Lushnikova, E., Nepomnyashchikh, L., Mazhbich, B., 1994. Quantitative ultrastructural analysis of rat cardiomyocytes during prolonged stay at high altitude. Byulleteń Eksp. Biol. i Meditsiny 117 (6), 661–665 (in Russian).
Malinovsky, G., Zhukovsky, M., Starichenko, V., Modorov, M., 2012. Nondestructive methods of ^{90}Sr content assessment in bones of mouse like rodents from East Ural radioactive trace. ANRI 70 (3), 87–92 (in Russian with English Abstract).
Malinovsky, G.P., Yarmoshenko, I.V., Zhukovsky, M.V., Starichenko, V.I., Chibiryak, M.V., 2014. Contemporary radiation doses to murine rodents inhabiting the most contaminated part of the EURT. J. Environ. Radioact. 129, 27–32.
Meyerson, F., 1981. Adaptation, Stress and Prevention. Nauka, Moskow (in Russian).
Molchanova, I., Pozolotina, V., Karavaeva, E., Mikhaylovskaya, L., Antonova, E., Antonov, K., 2009. Radioactive inventories within the East-Ural radioactive state reserve on the Southern Urals. Radioprotection 44 (5), 747–757.
Molchanova, I., Mikhailovskaya, L., Antonov, K., Pozolotina, V., Antonova, E., 2014. Current assessment of integrated content of long-lived radionuclides in soils of the head part of the east ural radioactive trace. J. Environ. Radioact. 138, 238–248.
Møller, A.P., Surai, P., Mousseau, T.A., 2005. Antioxidants, radiation and mutation as revealed by sperm abnormality in barn swallows from Chernobyl. Proc. R. Soc. 272, 247–253.
Mukhacheva, S.V., Davydova, Yu.A., Kshnyasev, I.A., 2010. Responses of small mammal community to environmental pollution by emissions from a copper smelter. Russ. J. Ecol. 41, 513–518.
Nepomnyashchikh, L., 1991. The Morphogenesis of the Major Pathological Processes in the Heart. Nauka, Sibirskoe otdelenie, Novosibirsk (in Russian).
Nurtdinova, D.V., Pyastolova, O.A., 2004. Ecological characteristics of small rodents living in collective gardens. Russ. J. Ecol. 35, 337–342.
Pentreath, P., 2002. Radiation protection of people and the environment: developing a common approach. J. Radiol. Prot. 22, 45–56.
Petin, V., Jin Kyu Kim, 2014. Synergistic Interaction and Cell Responses to Environmental Factors. Nova Science Publishers, USA.
Roe, J., Papadopoulos, N., 1954. The determination of fructose-6-phosphate and fructose 1,6-diphosphate. J. Biol. Chem. 210, 703–707.
Rogovin, K., Moshkin, M., 2007. Autoregulation in mammalian populations and stress: an old theme revisited. Zhurnal Obshchei Biol. 68 (4), 244–267 (in Russian with English Abstract).
Schneider, C.W., 1948. Intracellular distribution of enzymes. I I I. The oxidation of octanoic acid by rat liver fractions. J. Biol. Chem. 176, 259–266.
Secades, P., Rodrigo, J.P., Hermsen, M., Alvarez, C., Suarez, C., Chiara, M.D., 2009. Increase in gene dosage is a mechanism of Hif—1alpha constitutive expression in head and neck squamous cell carcinomas. Genes Chromosom. Cancer 48, 441–454.
Shpońka, I., 1996. Histo-genetic Processes in the Developing Mammalian Myocardium. Izdatelstvo "porogi, Dnepropetrovsk (in Russian).
Skulachev, V., 1989. Bioenergy. Membrane Converters. Vysshaya shkola, Moskow (in Russian).
Smith, J.T., Willey, N.J., Hancock, J.T., 2012. Low dose ionizing radiation produces too few reactive oxygen species to directly affect antioxidant concentrations in cells. Biol. Lett. 8 (4), 594–597.
Starichenko, V.I., Modorov, M.V., 2013. β-activity distribution in mouse-like rodents inhabiting East Urals radioactive trace. Radiat. Saf. Probl. Spec. Issue 66–73 (in Russian with English Abstract).
Starichenko, V., Lyubashevskiy, N., Modorov, M., Chibiryak, M., 2014. Skeletal ^{90}Sr as a marker of migration activity of murine rodents in the zone of the Eastern Ural radioactive trace. Russ. J. Ecol. 45 (3), 232–242.
StatSoft, Inc, 2012. Electronic Textbook on Statistics. Moskow. WEB: http://www.statsoft.ru/home/textbook/default.htm.
UNSCEAR. United Nations Scientific Committee on the Effects of Atomic Radiation, 1993. Sources and Effects of Ionizing Radiation. Report to the General Assembly, with Scientific Annexes. United Nations, New York.
UNSCEAR, 2008. United Nations. Sources and Effects of Ionizing Radiation. Volume II. Effects. Scientific Annexes C, D and E. UNSCEAR 2008 Report. United Nations Scientific Committee on the Effects of Atomic Radiation. United Nations sales publication E.11.IX.3. United Nations, New York, p. 2011.
Weiss, R., Chacko, V., Gerstenblith, G., 1989. Fatty acid regulation of glucose metabolism in the intact beating ret heart assessed by carbon13 NMR spectroscopy the critical role of dehydrogenase. J. Mol. Cell. Cardiol. 21, 469–478.
Yarmonenko, S., 1984. Radiobiology of Man and Animals. Vyshaya skola, Moscow (in Russian).
Yu, Z., Zhang, L., 1996. Effect of simulated weightlessness on ultrastructures and oxygen supply and consumption of myocardium in rats. Space Med. Med. Eng. 9 (4), 261–266.